Paper
Int'l J. of Aeronautical & Space Sci. 17(2), 195–203 (2016)
DOI: http://dx.doi.org/10.5139/IJASS.2016.17.2.195

IJASS
International Journal of Aeronautical and Space Sciences

H infinity control design for Eight-Rotor MAV attitude system based on identification by interval type II fuzzy neural network

Xiangjian CHEN*

School of computer science and Engineering, Jiangsu university of science and technology, Zhenjiang, Jiangsu 212003, China.

Kun SHU and Di LI*****

China Shipbuilding Industry corporation 723, Kunminghu Nan Lu, Haidian District, Beijing 100097, China.

Abstract

In order to overcome the influence of system stability and accuracy caused by uncertainty, estimation errors and external disturbances in Eight-Rotor MAV, L2 gain control method was proposed based on interval type II fuzzy neural network identification here. In this control strategy, interval type II fuzzy neural network is used to estimate the uncertainty and non-linearity factor of the dynamic system, the adaptive variable structure controller is applied to compensate the estimation errors of interval type II fuzzy neural network, and at last, L2 gain control method is employed to suppress the effect produced by external disturbance on system, which is expected to possess robustness for the uncertainty and non-linearity. Finally, the validity of the L2 gain control method based on interval type II fuzzy neural network identifier applied to the Eight-Rotor MAV attitude system has been verified by three prototy experiments.

Key words: interval type II fuzzy neural network, Eight-Rotor MAV, variable structure control, L2 gain control.

1. Introduction

Numerous applications of UAVs have been steadily increasing such as traffic surveillance, air pollution monitoring, area mapping, agricultural applications as well as remote inspection required high maneuverability. The merit of UAVs is maximized for the practical uses where it is dangerous and difficult to approach. For these reasons, quad-rotor UAVs [1-5] have evoked a great interest in the research and academic circles in recent years.

The coaxial Eight-Rotor[6,7] is designed with eight rotors that are arranged as four counter-rotating offset pairs mounted at the ends of four carbon fiber arms in a cruciform cofiguration.

As a result, the coaxial eight-rotor has twice overall thrust than a quad-rotor without increasing double weight. Obviously, the higher coefficient proportion between thrust and gravity and the greater payload capacity than a quad-rotor are provided by the eight-rotor. The frame of the coaxial eight-rotor is built from high quality military grade carbon fibre making it one of the most durable electric helicopters on the market today. During flight with carbon fibre. In addition, the eight-rotor could remain stable flight when some of rotors broken. If one rotor is broken, another in pairs will compensate the thrust reduced caused by the broken rotor, which is not provided in a quad-rotor.

Eight-Rotor MAV is nonlinear plant so that it is difficult to obtain stable control due to uncertainties. The purpose of this paper is to propose one robust, stable attitude control strategy for Eight-Rotor MAV to accommodate system uncertainties, variations, and external disturbances. The control strategy is based on Neuro-Fuzzy adaptive controller, Neuro-Fuzzy has been used in a lot of successful applications [8-11], But which is based on type-I fuzzy sets. With the higher control accuracy requirements, type-II fuzzy neural network [12,13] is developed recently which has

* Ph. D., Corresponding author: cxj831209@163.com
** kshu723@sina.com
*** lee_di@163.com

Received: September 9, 2014 Revised: December 19, 2015 Accepted: June 10, 2016

http://ijass.org pISSN: 2093-274x eISSN: 2093-2480

better performances than type-I fuzzy neural network. This paper is to apply type-II fuzzy neural networks to control the attitude of the Eight-Rotor MAV. More recently, there are many papers discussing how to improve the stability of fuzzy-neural controllers. It is well known that sliding mode control provides a robust means for controlling a nonlinear dynamic system with uncertainties, one gain adaptive sliding mode controller based on interval type-II fuzzy neural network [14-16] identification and Lyapunov synthesis approach for Eight-Rotor MAV which is MIMO nonlinear system. By introducing interval type-II fuzzy neural network to approximate the unknown nonlinear functions of the dynamic systems through tuning by the desired adaptive law.

H infinity control has stronger inhibition to the unknown interference, and L2 gain design method is the most common method in the H infinity control of nonlinear system. Combining the characteristics of the adaptive control, variable structure control and H infinity control applied in the nonlinear system, this paper proposed L2 gain control method based on interval type II fuzzy neural network identifier.

This paper is organized as follows: The attitude dynamic model of EightRotor MAV are given in Section 2. A brief illustration of interval type-II fuzzy neural network is presented in Section 3. L2 gain control method based on interval type II fuzzy neural network identifier is constructed in Section 4. which is also devoted to the stability analysis of the control scheme. Platform description and some experiences are given in Section 5 and Section 6 contains concluding remarks.

2. Dynamic modeling of attitude for Eight-Rotor MAV

The EightRotor is very well modeled with eight rotors in a cross configuration. This cross structure is quite thin and light, however it shows robustness by linking mechanically the motors. Each propeller is connected to the motor through the reduction gears. All the propellers axes of rotation are fixed and parallel. These considerations point out that the structure is quite rigid and the only things that can vary are the propeller speeds. Neither the motors nor the reduction gears are fundamental because the movements are directly related just to the propellers velocities can be seen in Fig. 1.

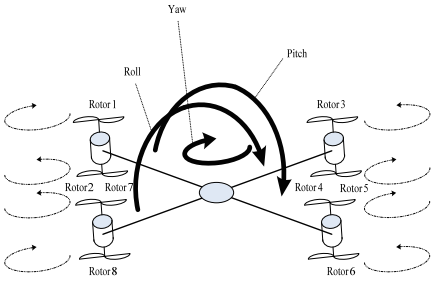

Fig. 1. Flight theory of Eight-Rotor MAV

Attitude angular velocity dynamic equation under torque U for Micro Aircraft Vehicle has been achieved in the body fixed frame according to the reference [1-3], which is given as following:

$$J\dot{w} = -\Omega Jw + U + d \tag{1}$$

Where $J \in R^{3\times3}$ denotes the rotational inertia matrix of Micro Aircraft Vehicle;

$w=[p,q,r]^T$ denotes the angular velocity of Micro Aircraft Vehicle; $U=[U_x,U_y,U_z]^T$ denotes the control torque in the body fixed frame; $d=[d_1,d_2,d_3]^T$ denotes the external disturbance torque, matrixes J, Ω, U are defined respectively as:

$$J=\begin{bmatrix} I_x & 0 & 0 \\ 0 & I_y & 0 \\ 0 & 0 & I_z \end{bmatrix}, \Omega=\begin{bmatrix} 0 & -r & -q \\ r & 0 & -p \\ -q & p & 0 \end{bmatrix}$$

$$U=\begin{pmatrix} U_x \\ U_y \\ U_z \end{pmatrix}=\begin{pmatrix} \rho AC_T R^2(\Omega_1^2+\Omega_2^2-\Omega_5^2-\Omega_6^2) \\ \rho AC_T R^2(\Omega_3^2+\Omega_4^2-\Omega_7^2-\Omega_8^2) \\ \rho AC_T R^2(\Omega_1^2-\Omega_2^2+\Omega_5^2-\Omega_6^2-\Omega_3^2+\Omega_4^2-\Omega_7^2+\Omega_8^2) \end{pmatrix} \tag{2}$$

Where ρ is air density, R denotes rotor radius, $A=\pi R^2$ is rotor disk area, and C_T, C_D express thrust coefficient and torque coefficient respectively. l represents the distance between the rotor and centre of the eight-rotor.

Organizing above equations, we obtain:

$$\begin{cases} \dot{p} = \dfrac{U_x - qr(I_z - I_y)}{I_x} \\ \dot{q} = \dfrac{U_y - pr(I_x - I_z)}{I_x} \\ \dot{r} = \dfrac{U_z - pq(I_y - I_x)}{I_z} \end{cases} \tag{3}$$

It is not difficult to obtain the relationship between attitude angular velocity and three angular velocity components in the body fixed frame through the transformation matrix between body fixed frame and earth fixed frame, the attitude angular dynamic equation is given as:

$$\begin{bmatrix} \dot{\phi} \\ \dot{\theta} \\ \dot{\psi} \end{bmatrix} = \begin{bmatrix} 1 & \sin\phi\tan\theta & \cos\phi\tan\theta \\ 0 & \cos\phi & -\sin\phi \\ 0 & \sin\phi/\cos\theta & \cos\phi/\cos\theta \end{bmatrix} \begin{bmatrix} p \\ q \\ r \end{bmatrix} \tag{4}$$

where ϕ, θ, ψ represent the roll, pitch and yaw angels in the inertial reference frame.

Making the outputs track the attitude of Eight-Rotor MAV by designing the control torque U. Arranging the above dynamic equations for designing the control scheme conveniently, the attitude control model of Micro Aircraft Vehicle obtained can be expressed as:

$$\begin{cases} \dot{x}_1 = bT \\ \dot{T} = F(T) + U + d \\ y = x_1 \end{cases} \tag{5}$$

Where $\varphi = [\theta \quad \psi \quad \phi]^T$, $w = [q \quad r \quad p]^T$,

$$F(T) = \left[\frac{(I_x - I_z)pr}{I_y} \quad \frac{(I_x - I_y)pq}{I_z} \quad \frac{(I_z - I_y)qr}{I_x} \right]^T,$$

$$U = [U_2 \quad U_3 \quad U_1]^T, b(x_1) = \begin{bmatrix} \cos\phi & -\sin\phi & 0 \\ \sin\phi/\cos\theta & \cos\phi/\cos\theta & 0 \\ \sin\phi\tan\theta & \cos\phi\tan\theta q & 1 \end{bmatrix}.$$

Next, propose $x=bT$, $f = \dot{b}F(T) + bT$, the control model turned to as following eventually:

$$\begin{cases} \ddot{x} = f + f_\Delta + (b + b_\Delta)U + d \\ y = x \end{cases} \tag{6}$$

where $x_1, x_2, x \in R^3$ denotes controlled state vector, $F, f \in R^3$ means system function vector, $b \in R^{3\times3}$ means control coefficient matrix, $U \in R^3$ means control input matrix vector, $d \in R^3$ means the disturbance vector, $y \in R^3$ means the control output vector, $f_\Delta, b_\Delta \in R^{3\times3}$ means uncertainty function vector caused by attitude perturbations, each component expression of $f=[f_1\ f_2\ f_3]^T$ referred to as:

$$\begin{cases} f_1 = (p + q\tan\theta\sin\phi + r\tan\theta\cos\phi)(-r\cos\phi - q\sin\phi) - \dfrac{I_x - I_y}{I_z} pq\sin\phi \\ \quad + \dfrac{I_z - I_x}{I_y} rp\cos\phi \\ f_2 = \dfrac{1}{\cos\theta}((p + q\tan\theta\sin\phi + r\tan\theta\cos\phi)(q\cos\phi - r\sin\phi) + \dfrac{I_x - I_y}{I_z} pq\sin\phi \\ \quad + \tan\theta(q\sin\phi + r\cos\phi)(q\sin\phi - r\cos\phi) + \dfrac{I_z - I_x}{I_y} rp\cos\phi) \\ f_3 = + \dfrac{I_y - I_z}{I_x} rq + \dfrac{I_x - I_y}{I_z} pq\cos\phi\tan\theta + \dfrac{I_z - I_x}{I_y} rp\sin\phi\tan\theta \\ \quad + \tan\theta(p + q\tan\theta\sin\phi + r\tan\theta\cos\phi)(q\cos\phi - r\sin\phi) \\ \quad + \dfrac{1}{\cos^2\theta}(q\sin\phi + r\cos\phi)(q\sin\phi - r\cos\phi) \end{cases} \tag{7}$$

Aerodynamic characteristics parameters will get perturbations resulting from flying conditions or flying attitude changed. At the same time, external gust of wind and flow could not be ignored. Thus, control system of Micro Aircraft Vehicle is one MIMO nonlinear system with uncertainty and perturbations.

3. Introduce of Interval Type-II Fuzzy Neural Network

The structure of ITIIFNN [16-17] is depicted in Fig. 2; each rule in ITIIFNN is the first Takagi-Sugeno-Kang (TSK) type. The detailed mathematical functions of each layer are introduced as follows:

Layer 1 (Input layer): This layer defines the input variables which first enter the ITIIFNN.

Layer 2 (Membership layer): In this layer, each node performs an interval type-II fuzzy MF. The FOU of this MF can be represented as an interval bound by lower MF $\underline{\mu}_i^j(x_i)$ and upper MF $\overline{\mu}_i^j(x_i)$:

$$\begin{aligned} \overline{\mu}_i^j(x_i) &= \begin{cases} N(\underline{\zeta}_i^j, \sigma_i^j, x_i), x_i < \underline{\zeta}_{j1}^i \\ 1, \qquad \underline{\zeta}_i^j \le x_i < \overline{\zeta}_i^j \\ N(\overline{\zeta}_i^j, \sigma_i^j, x_i), x_i > \overline{\zeta}_i^j \end{cases} \\ \underline{\mu}_i^j(x_i) &= \begin{cases} N(\underline{\zeta}_i^j, \sigma_i^j, x_i), x_j \le \dfrac{\underline{\zeta}_i^j + \overline{\zeta}_i^j}{2} \\ N(\overline{\zeta}_i^j, \sigma_i^j, x_i), x_j > \dfrac{\underline{\zeta}_i^j + \overline{\zeta}_i^j}{2} \end{cases} \end{aligned} \tag{8}$$

Where $\zeta_i^j \in [\underline{\zeta}_i^j, \overline{\zeta}_i^j]$ and σ_i^j are, respectively, the mean and the standard deviation of the Gaussian MF of the jth partition for the ith input variable x_i. That is, the output of each node can be represented as an interval $[\underline{\mu}_i^j, \overline{\mu}_i^j]$.

Layer 3 (Rule layer): Each node in this layer corresponds to one fuzzy rule and performs a fuzzy meet operation to obtain a firing strength F^i which is computed as follows:

$$F^i = [\underline{f}^i, \overline{f}^i] = [\prod_{j=1}^{n} \overline{\mu}_{ji}, \prod_{j=1}^{n} \underline{\mu}_{ji}] \tag{9}$$

Layer 4 (Type-reduction layer): This layer is used to implement the type-reduction, and center-of-sets type-reduction method is adopted here. The centroid of type-II fuzzy set which can be represented by $[\omega_l^j, \omega_r^j]$ which represents link weights should be set first before the computation of y_l, y_r. The outputs y_l, y_r can be computed using Kamik-Mendel iterative algorithms as:

$$y_l = \frac{\sum_{j=1}^{L} \underline{f}^j w_l^j + \sum_{j=L+1}^{N} \overline{f}^j w_l^j}{\sum_{j=1}^{L} \underline{f}^j + \sum_{j=L+1}^{N} \overline{f}^j} = W_l^T g_l \tag{10}$$

$$y_r = \frac{\sum_{j=1}^{R} \underline{f}^j w_r^j + \sum_{j=R+1}^{N} \overline{f}^j w_r^j}{\sum_{j=1}^{R} \underline{f}^j + \sum_{j=R+1}^{N} \overline{f}^j} = W_r^T g_r \tag{11}$$

Where $W_r = [\omega_r^1, \cdots, \omega_r^N]^T$, $W_l = [\omega_l^1, \cdots, \omega_l^N]^T$ and

$$g_l = \left[\frac{f_l^1}{\sum_{i=1}^{N} f_l^i}, \frac{f_l^2}{\sum_{i=1}^{N} f_l^i}, \cdots, \frac{f_l^N}{\sum_{i=1}^{N} f_l^i} \right]^T$$
$$g_r = \left[\frac{f_r^1}{\sum_{i=1}^{N} f_r^i}, \frac{f_r^2}{\sum_{i=1}^{N} f_r^i}, \cdots, \frac{f_r^N}{\sum_{i=1}^{N} f_r^i} \right]^T \quad (12)$$

Layer 5 (Output layer): Each output node corresponds to one output variable and act as a defuzzifier. Hence, the defuzzified output shown as:

$$y = \frac{y_l + y_r}{2} = \frac{1}{2}(W_l^T g_l + W_r^T g_r) = W^T g(x, \zeta, \sigma) \quad (13)$$

Remark : Initially, there are no fuzzy rules in ITIIFNN. All of the rules are generated online by the structure learning that not only helps automate rule generation, but also locates good initial rule positions for subsequent parameter learning. Furthermore, the structure and parameter adjustment are performed simultaneously.

4. L2-ITIIFNN

To begin with, ITIIFNN as shown in Fig. 2 is used to estimate the uncertainty factors, and also evaluate the bounds of the modeling error in order to determine the gain of variable structure control and achieve the real variable structure control vector, which make sure that the system obtained not only the robustness of estimation errors, but also the smaller chatter. L2 gain control method is employed to suppress the effect produced by external disturbance on system, which is expected to possess robustness for the uncertainty and non-linearity. Then, analyzing the stability of the proposed control strategy through Lyapuno stability theorem.

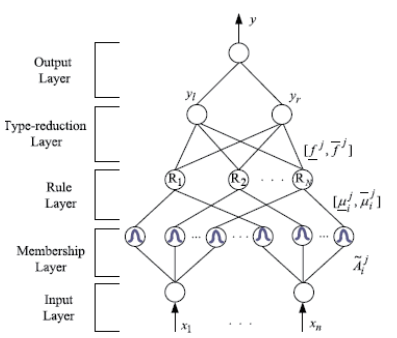

Fig. 2. The structure of IT-IIFNN

4.1 Controller Design

Proposing y_d is the desired trajectory, and define

$$E = [e, \dot{e}, \ddot{e}, \cdots, e^{(n-1)}]^T = [y_d - y, \dot{y}_d - \dot{y}, \cdots, y_d^{(n-1)} - y^{(n-1)}]^T$$

Then the error dynamic equation with uncertainty and external disturbances can be expressed as:

$$\dot{E} = AE + B\{k^T E + y_d^{(n)} - f_0 - \hat{f}_\Delta - (b_0 + \hat{b}_\Delta)u - d\} \quad (14)$$

Where,

$$A = \begin{bmatrix} 0 & 1 & 0 & 0 & \cdots & 0 & 0 \\ 0 & 0 & 1 & 0 & \vdots & 0 & 0 \\ \vdots & \vdots & \vdots & \vdots & \vdots & \vdots & \vdots \\ 0 & 0 & 0 & 0 & 0 & 0 & 1 \\ -k_n & -k_{n-1} & -k_{n-2} & -k_{n-3} & \cdots & -k_2 & -k_1 \end{bmatrix} B = \begin{bmatrix} 0 \\ 0 \\ \vdots \\ 0 \\ 1 \end{bmatrix} \quad (15)$$

In the meantime, the selection of $k=[k_n, k_{n-1}, ..., k_1]^T$ should make sure that $s^n + k_1 s^{n-1} + ... + k_n$ is Hurwitz polynomial.

Taking $x=[\phi, \theta, \psi]^T$ as the input of the ITIIFNN to approximate the uncertainty function f and nonlinear function b on-line. We replace f and b by ITIIFNN as:

$$\hat{f}_\Delta(x \mid \vartheta_{f\Delta}) = W_{f\Delta}^T g_{f\Delta}(x, \zeta, \sigma)$$
$$\hat{b}_\Delta(x \mid \vartheta_{b\Delta}) = W_{b\Delta}^T g_{b\Delta}(x, \zeta, \sigma) \quad (16)$$

And propose that $f_\Delta^* = \hat{f}_\Delta(x \mid \vartheta_{f\Delta}^*), b^* = \hat{b}_\Delta(x \mid \vartheta_{b\Delta}^*)$ respect to the optimal estimations of $f_\Delta(x)$, $b_\Delta(x)$, the minimum estimation error is defined as:

$$f_\Delta^* - f_\Delta = E_{f\Delta}, b_\Delta^* - b_\Delta = E_{b\Delta} \quad (17)$$

Where $\vartheta_\#$ respects to adjustable parameters including the Gaussian membership function mean $\zeta_i^j \in [\underline{\zeta}_i^j, \overline{\zeta}_i^j]$, Gaussian membership function standard deviation σ_i^j, neural network weight $[W_l^j, W_r^j]$, # means $f_\Delta(x)$ and $b_\Delta(x)$. Then, expand $\hat{f}_\Delta(x \mid \vartheta_{f\Delta}^*)$ and $\hat{b}_\Delta(x \mid \vartheta_{b\Delta}^*)$ in the Taylor series expression near :

$$\hat{f}_\Delta(x \mid \vartheta_{f\Delta}) - \hat{f}_\Delta(x \mid \vartheta_{f\Delta}^*) = \Phi_{f\Delta}^T \left(\frac{\partial \hat{f}_\Delta(x \mid \vartheta_{f\Delta})}{\partial \vartheta_{f\Delta}} \right) + O(|\Phi_{f\Delta}|^2)$$
$$\hat{b}_\Delta(x \mid \vartheta_{b\Delta}) - \hat{b}_\Delta(x \mid \vartheta_{b\Delta}^*) = \Phi_{b\Delta}^T \left(\frac{\partial \hat{b}_\Delta(x \mid \vartheta_{b\Delta})}{\partial \vartheta_{b\Delta}} \right) + O(|\Phi_{b\Delta}|^2) \quad (18)$$

Where $\Phi_{f\Delta} = \vartheta_{f\Delta} - \vartheta_{f\Delta}^*$, $\Phi_{b\Delta} = \vartheta_{b\Delta} - \vartheta_{b\Delta}^*$, $\dot{\Phi}_{b\Delta} = \dot{\vartheta}_{b\Delta}$ and are $O(|\Phi_{f\Delta}|^2), O(|\Phi_{b\Delta}|^2)$ representative to the higher-order

item. Each item of $\frac{\partial \hat{f}_\Delta(x|\vartheta_{f\Delta})}{\partial \vartheta_{f\Delta}}$ is expressed as:

$$\begin{aligned}
&\frac{\partial \hat{f}_\Delta}{\partial w_{lr}^j}|_k=\frac{\bar{y}_{f\Delta}^j-\hat{f}_\Delta}{\sum_{j=1}^N f_{lr}^j}\times f_{lr}^j\\
&\frac{\partial \hat{f}_\Delta}{\partial \underline{\zeta}_i^j}|_k=\frac{\frac{1}{2}\frac{\bar{y}_{f\Delta}^j-\hat{f}_\Delta}{\sum_{j=1}^N f_{lr}^j}\left[\frac{w_{lr}^j-y_{lr}}{\sum_{j=1}^N f_{lr}^j}*\left(x(k-1)-\underline{\zeta}_i^j(k-1)\right)\right]\times \underline{f}^j}{\left(\sigma_i^j(k-1)\right)^2}\\
&\frac{\partial \hat{f}_\Delta}{\partial \bar{\zeta}_i^j}|_k=\frac{\frac{1}{2}\frac{\bar{y}_{f\Delta}^j-\hat{f}_\Delta}{\sum_{j=1}^N f_{lr}^j}\left[\frac{w_{lr}^j-y_{lr}}{\sum_{j=1}^N f_{lr}^j}*\left(x(k-1)-\bar{\zeta}_i^j(k-1)\right)\right]\times \bar{f}^j}{\left(\sigma_i^j(k-1)\right)^2}\\
&\frac{\partial \hat{f}_\Delta}{\partial \sigma_{f\Delta}^j}|_k=\frac{\frac{1}{2}\frac{\bar{y}_{f\Delta}^j-\hat{f}_\Delta}{\sum_{j=1}^N f_{lr}^j}\left[\frac{w_{lr}^j-y_{lr}}{\sum_{j=1}^N f_{lr}^j}*\left(x(k-1)-\bar{\zeta}(k-1)^2\right)\right]\times f_{lr}^j}{\left(\sigma_i^j(k-1)\right)^3}
\end{aligned} \tag{19}$$

Replacing the $f_\Delta(x)$ with $b_\Delta(x)$, $\frac{\partial \hat{b}_\Delta(x|\vartheta_{b\Delta})}{\partial \vartheta_{b\Delta}}$, can be achieved. Hence, we obtain:

$$\begin{aligned}
&\hat{f}_\Delta-f_\Delta=\hat{f}_\Delta-f_\Delta^*+f_\Delta^*-f_\Delta=\Phi_{f\Delta}^T(\frac{\partial \hat{f}_\Delta}{\partial \vartheta_{f\Delta}})+O(|\Phi_{f\Delta}|^2)+E_{f\Delta}\\
&\hat{b}_\Delta-b_\Delta=\hat{b}_\Delta-b_\Delta^*+b_\Delta^*-b_\Delta=\Phi_{b\Delta}^T(\frac{\partial \hat{b}_\Delta}{\partial \vartheta_{b\Delta}})+O(|\Phi_{b\Delta}|^2)+E_{b\Delta}
\end{aligned} \tag{20}$$

Then,

$$\begin{aligned}
&-f_\Delta=-\hat{f}_\Delta+\Phi_{f\Delta}^T(\frac{\partial \hat{f}_\Delta}{\partial \vartheta_{f\Delta}})+O(|\Phi_{f\Delta}|^2)+E_{f\Delta}\\
&-b_\Delta=-\hat{b}_\Delta+\Phi_{b\Delta}^T(\frac{\partial \hat{b}_\Delta}{\partial \vartheta_{b\Delta}})+O(|\Phi_{b\Delta}|^2)+E_{b\Delta}
\end{aligned} \tag{21}$$

If the estimation error is zero, the control vector is:

$$u_c=\frac{-f_0(x)-\hat{f}_\Delta(x)+y_d+k^TE+u_L}{b_0(x)+b_\Delta(x)} \tag{22}$$

$$u_L=-B^TPE/r \tag{23}$$

Where r means the robust control gain. Meanwhile, variable structure control vector is drowned in the system, in order to compensate the estimation errors based on ITIIFNN, and enhance the robustness of the system, variable structure control :

$$u_s=-\hat{K}_{vc}^T\varphi\,\mathrm{sgn}(E^TPB)/\beta \tag{24}$$

Then, the total control is shown as follow

$$u=u_c+u_s \tag{25}$$

4.2 stability analysis

Theorem 1. Consider the dynamic system Eq. (23), ρ>0 is given, hypothesizing $b(x)\geq\beta$>0, and existing the positive definite symmetric matrix P, which satisfied the Riccati equation as shown:

$$PA+A^TP+Q+PB(\frac{1}{\rho^2}-\frac{2}{r})B^TP=0$$

In the above equation: $Q=Q^T$>0,which serves as weight matrix, ρ>0,which serves as specified against standard, ρ, r has to be satisfy the following inequality, to ensure that the Riccati equation with semi positive definite solution:

$$2\rho^2\geq r$$

The adjustable parameters adaptive laws of ITIIFNN and gain adaptive laws of variable structure control are chosen as:

$$\dot{\vartheta}_{f\Delta}=-\Gamma_{f\Delta}E^TPB\frac{\partial \hat{f}_\Delta}{\partial \vartheta_{f\Delta}} \tag{26}$$

$$\dot{\vartheta}_{b\Delta}=-\Gamma_{b\Delta}E^TPB\frac{\partial \hat{b}_\Delta}{\partial \vartheta_{b\Delta}} \tag{27}$$

$$\dot{\hat{K}}_{vc}=\Gamma_{kvc}\left|E^TPB\right|\varphi \tag{28}$$

Where $\Gamma_{f\Delta}>0,\Gamma_{b\Delta}>0,\Gamma_{Kvc}>0$ denote the adaptive gain matrixes. then, the control vector u determined by Eq.(22)-(25), which can make the dynamic system Eq.(6) with the

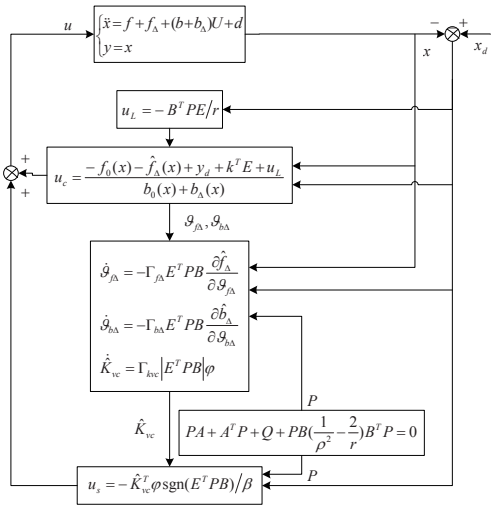

Fig. 3. Architecture of L2 gain control method based on ITIIFNN identifier

following characteristics:

(1). When the system is stable, d=0, for arbitrary initial states, the following equation is proved:

$$\lim_{t\to\infty} E(t) = \lim_{t\to\infty} x_d(t) - x(t) = 0$$

(2). When $d\neq 0$, for arbitrary initial states, and $V(0)$=0, the following equation is proved:

$$\int_0^T \|z\|^2 dt \le \rho^2 \int_0^T \|d(t)\|^2 dt$$

Proof: As a result of $\dot{e}_n = y_d - \dot{x}_n$, combining the control vector Eq.(25) and dynamic system Eq.(6), then, the error dynamic equation could be achieved as:

$$\dot{E} = AE + B\{(\hat{f}_\Delta - f_\Delta^*) + (f_\Delta^* - f_\Delta) + [(\hat{b}_\Delta - b_\Delta^*) + (b_\Delta^* - b_\Delta)]u_c - d + u_L - (b_0 + b_\Delta)u_s\} \quad (29)$$

Define a Lyapunov function as:

$$V = \frac{1}{2}E^T PE + \frac{1}{2}\Phi_{f\Delta}^T \Gamma_{f\Delta}^{-1}\Phi_{f\Delta} + \frac{1}{2}\Phi_{b\Delta}^T \Gamma_{b\Delta}^{-1}\Phi_{b\Delta} + \frac{1}{2}\tilde{K}_{vc}\Gamma_{Kvc}^{-1}\tilde{K}_{vc}$$

Then, the differential time of the above V along the dynamical equation Eq. (29) shown as:

$$\begin{aligned}\dot{V} &= \frac{1}{2}\dot{E}^T PE + \frac{1}{2}E^T P\dot{E} + \Phi_{f\Delta}^T \Gamma_{f\Delta}^{-1}\dot{\Phi}_{f\Delta} + \Phi_{b\Delta}^T \Gamma_{b\Delta}^{-1}\dot{\Phi}_{b\Delta} + \tilde{K}_{vc}\Gamma_{Kvc}^{-1}\dot{\tilde{K}}_{vc} \\ &\le -\frac{1}{2}E^T(A^T P + AP^T)E + |E^T PB|(\varepsilon_f + \varepsilon_b |u_c|) - bu_s E^T PB + (u_L - d)B^T PE + \\ &\quad E^T PB(\Phi_{f\Delta}^T \frac{\partial \hat{f}_\Delta}{\partial \theta_{f\Delta}} + \Phi_{b\Delta}^T \frac{\partial \hat{b}_\Delta}{\partial \theta_{b\Delta}}) + \Phi_{f\Delta}^T \Gamma_{f\Delta}^{-1}\dot{\theta}_{f\Delta} + \Phi_{b\Delta}^T \Gamma_{b\Delta}^{-1}\dot{\theta}_{b\Delta} + \tilde{K}_{vc}\Gamma_{Kvc}^{-1}\dot{\tilde{K}}_{vc}\end{aligned}$$

Substituting the adaptive law Eq. (26) and Eq. (17), $K_{vc}^* = [\varepsilon_{f\Delta} \quad \varepsilon_{b\Delta}]^T, \varphi = [1 \quad |u_c|]^T$, the above formula could be converted into:

$$\dot{V} \le -\frac{1}{2}E^T(A^T P + AP^T)E + + |E^T PB| K_{vc}^{*T}\varphi - bu_s E^T PB - (E^T PB\frac{1}{r} + d)B^T PE + \tilde{K}_{vc}\Gamma_{Kvc}^{-1}\dot{\tilde{K}}_{vc}$$

Substituting the control vector Eq.(24), and simplified, then get:

$$\begin{aligned}\dot{V} &\le -\frac{1}{2}E^T(A^T P + AP^T)E + + |E^T PB| K_{vc}^{*T}\varphi - \frac{b}{\beta}\hat{K}_{vc}^T\varphi \mathrm{sgn}(E^T PB)E^T PB \\ &\quad -(E^T PB\frac{1}{r} + d)B^T PE + \tilde{K}_{vc}\Gamma_{Kvc}^{-1}\dot{\tilde{K}}_{vc} \\ &\le -\frac{1}{2}E^T(A^T P + AP^T)E + + |E^T PB| K_{vc}^{*T}\varphi - \hat{K}_{vc}^T\varphi \mathrm{sgn}(E^T PB)E^T PB \\ &\quad -(E^T PB\frac{1}{r} + d)B^T PE + \tilde{K}_{vc}\Gamma_{Kvc}^{-1}\dot{\tilde{K}}_{vc} \\ &= -\frac{1}{2}E^T(A^T P + AP^T)E + + |E^T PB| \tilde{K}_{vc}^T\varphi - (E^T PB\frac{1}{r} + d)B^T PE + \tilde{K}_{vc}\Gamma_{Kvc}^{-1}\dot{\tilde{K}}_{vc}\end{aligned}$$

Subsitituting the adptive law Eq.(28), then get:

$$\begin{aligned}\dot{V} &\le \frac{1}{2}E^T(A^T P + AP^T)E - E^T PB\frac{1}{r}B^T PE + \\ &\quad \frac{1}{2}E^T PB\frac{1}{\rho^2}B^T PE - \frac{1}{2}E^T PB\frac{1}{\rho^2}B^T PE - dB^T PE - \frac{1}{2}\rho^2 d^2 + \frac{1}{2}\rho^2 d^2 \\ &= \frac{1}{2}E^T[A^T P + AP^T + PB(\frac{1}{\rho^2} - \frac{2}{r})B^T P]E - \frac{1}{2}(\frac{1}{\rho^2}B^T PE + \rho d)^2 + \frac{1}{2}\rho^2 d^2 \\ &\le -\frac{1}{2}E^T QE + \frac{1}{2}\rho^2 d^2\end{aligned}$$

Let's assume:

$$z = Q^{\frac{1}{2}}E \ , \ w(t) = d(t)$$

Obtaining the integral interval on the both sides of the above formula, and using $V(0)$=0, then:

$$0 \le V(t) \le \frac{1}{2}(\rho^2 \int_0^T \|w\|^2 dt - \int_0^T \|z\|^2 dt)$$

Therefore, for any disturbance input $w(t)$, $\|z\|_T \le \rho\|w\|_T$ is true. So the proposition (2) of the theorem 1 has been proved.

When, $d(t)$=0, for the quasi positive definite function V:

$$\dot{V} \le -\frac{1}{2}E^T QE$$

According the Lyapunov stability theory, for any initial state $x(0)=x_0$, the dynamical system is asymptotically stable, as:

$$\lim_{t\to\infty} E(t) = 0$$

Theorem 1 has been proved.

5. Experimental setup

The Eight-Rotor MAV prototype is designed with high quality military grade carbon fibre in a cruciform cofiguration. It has four pairs of blades driven by eight Brushless Direct Current (BLDC) motors mounted at each end of the body frame, as shown in Fig. 4. Its empty weight 1.6kg with payload capacity about 0.5kg can permit 30min flight duration.

Figure 5 presents the schematic view of aerial control platform. It uses TMS320F2812(DSP) which runs at 29.4MHz, with 512k flash memory, including eight serial ports, eight channels with programmable gains, 24-bit analog input, eight programmable pulse width modulation (PWM) outputs, and supports floating point calculations as the on-board flight control computer. A low-cost IMU which includes accelerometers, gyroscopes as well as

Fig. 4. The Eight-Rotor prototype MAV

magnetometers in 3D and a distance laser sensor are installed on the prototype to measure the flight states. IMU transmits raw data at sampling frequency of 100Hz and the distance laser sensor at sampling frequency of 7Hz with the accuracy of ±1.5mm. These sensor dates are transmitted to the on-board flight control computer through an RS-232 serial port. And the on-board computer can export these dates through wireless transfer module to the host computer which will arrange the dates and generate the corresponding schematic diagrams.

For avoiding signal interference between sensor signals and the motors PWM, two independent power supplies were supplied. One battery is used to feed the eight electric motors which are controlled using PWM, the other battery is used to feed microcontroller and the sensors, and by adequate grounding, the interference is reduced largely.

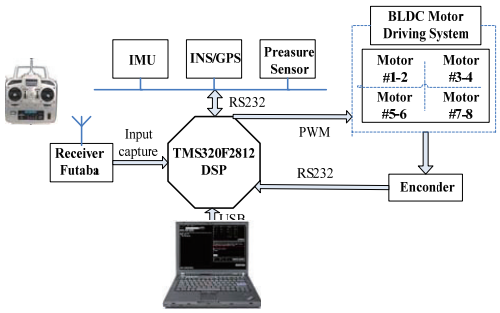

Fig. 5. Schematic view of aerial control platform using TMS320F2812

6. Experimental results

The Eight-rotor prototype MAV can successfully accomplish remote control flight task. For the purpose of comparison, several different kinds of control scheme are conducted to demonstrate the effectiveness of the proposed approach. We will apply type-I fuzzy neural network based sliding mode controller and interval type-II fuzzy neural network identification based gain adaptive sliding mode controller and L2 gain method based on interval type II fuzzy

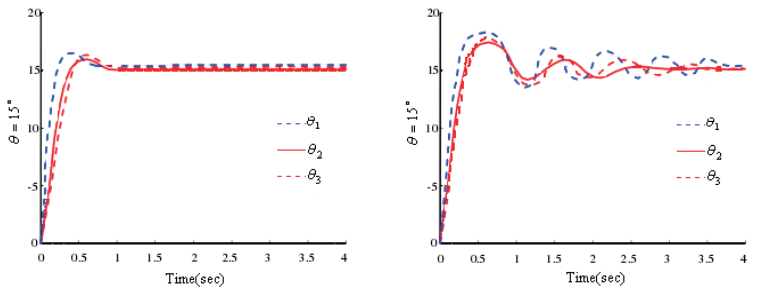

(a) Response curves of pitch angle θ

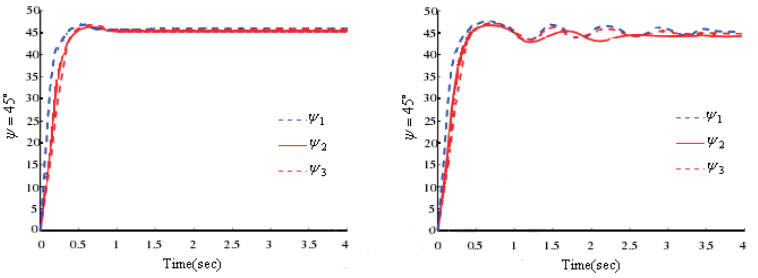

(b) Response curves of yaw angle ψ

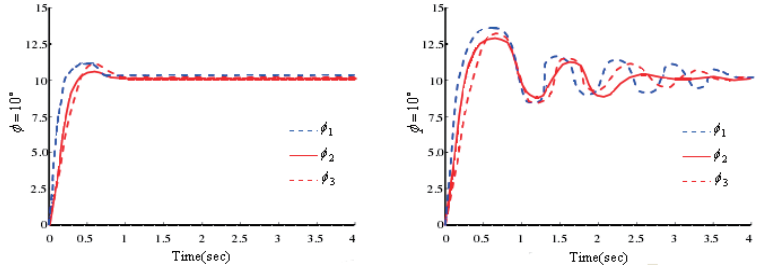

(c) Response curves of roll angle ϕ

Fig. 6. Response curves of attitude angles

neural network identifier to let the Eight-rotor prototype MAV system to track the reference attitude trajectory. Then, the comparison was preceded in the following cases:

Case 1 no wind disturbance indoors

Three attitude angles of trajectory tracking simulations have been made as follows: Fig.6 shows the trajectory tracking response curve of three angles and the trajectory tracking error curves of yaw angle under the circumstance without external disturbance and uncertainty.

Subscript Numbers under attitude Angles corresponding to three kinds of controller: "1" is a representative of type-I fuzzy neural network based sliding mode controller; "2" is a representative of interval type-II fuzzy neural network identification based gain adaptive sliding mode controller; "3" is a representative of L2 gain method based on interval type II fuzzy neural network identifier.

The above experimental results indicate that tracking performances can be guaranteed under three different control scheme without uncertainty and external disturbances. Type-1 fuzzy neural network based sliding mode control scheme which responses fast, but its overshoot is somewhat of big; interval type-II fuzzy neural network identification based gain adaptive sliding mode control scheme which has smaller steady-state error, but with longer regulation time; L2 gain method based on interval type II fuzzy neural network identifier control scheme which has better control accuracy and smaller overshoot.

Case 2 horizontal wind disturbance with average speed of 5m/s provided by the electric fan indoors

Figure 8 shows the trajectory tracking response curve of three attitude angles and the trajectory tracking error curves of yaw angle under the circumstance with external disturbance and uncertainty.

Subscript Numbers under attitude Angles corresponding to three kinds of controller: "1" is a representative of type-I fuzzy neural network based sliding mode controller; "2" is a representative of interval type-II fuzzy neural network identification based gain adaptive sliding mode controller; "3" is a representative of L2 gain method based on interval type II fuzzy neural network identifier.

From the above simulation results from Fig. 6 - Fig. 9. we can see that the control accuracy decreased under uncertainty

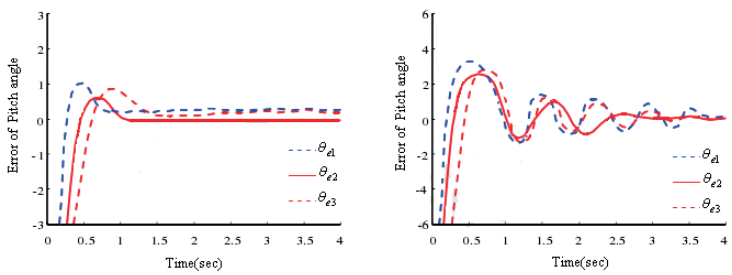

(a) Tracking error curves of Pitch angle θ

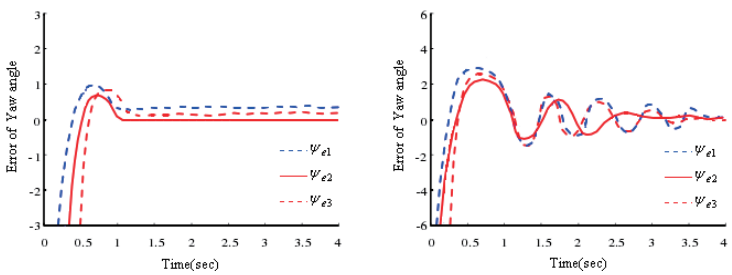

(b) Tracking error curves of Yaw angle ψ

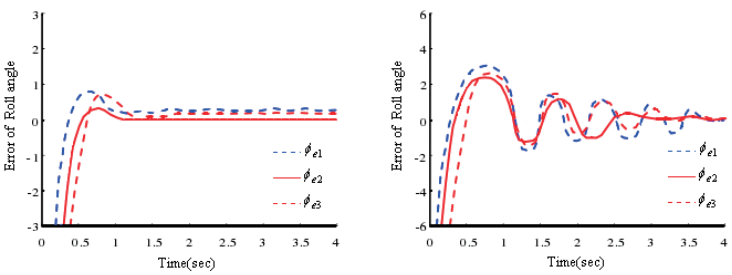

(c) Tracking error curves of Roll angle ϕ

Fig. 7. Tracking error curves of attitude angles

DOI: http://dx.doi.org/10.5139/IJASS.2016.17.2.195

factors and external disturbances for all of the three control schemes, but which could satisfy the performance standard of control system, furthermore, the L2 gain method based on interval type II fuzzy neural network identifier control scheme gives better performances compared with the other ones.

7. Conclusion

This paper develops a novel coaxial eight-rotor UAV to address the issue of weak movement capacity of a quad-rotor UAV. Owing to its structural characteristics, the eight-rotor offers remarkable advantages with respect to increased yaw movement ability, greater payload capacity and damage tolerance over a quad-rotor. Finally, numerical eight-rotor prototype comparison experiments indoors between L2 gain method based on interval type II fuzzy neural network identifier control scheme, type-I fuzzy neural network based sliding mode control scheme and interval type-II fuzzy neural network identification based gain adaptive sliding mode control scheme have been conducted. The results show three strategies adopted to the eight-rotor as the yaw controller have the good performance in the absence of the external disturbance and uncertainty. While in the case of external disturbances and uncertainty, it is evident that L2 gain method based on interval type II fuzzy neural network identifier control method is better suited in the yaw movement of the eight-rotor with more accurate control performance and stronger robustness.

Acknowledgement

This paper is supported by National Natural Science Found of China No.61502211

References

[1] Pounds, P., Mahony, R., Hynes, P. and Roberts, J. M., "Design of a Four-rotor Aerial Robot", *Proceedings of Australian Conference on Robotics and Automation*, 2002, pp. 145-150.

[2] McKerrow, P., "Modelling the Draganflyer Four-rotor Helicopter", *Proceedings of the IEEE International Conference on Robotics and Automation*, 2004, pp. 3596-3601.

[3] Bouabdallah, S., Noth, A. and Siegwart, R., "PID vs. LQ Control Techniques Applied to an Indoor Micro Quadrotor", *IEEE International Conference on Intelligent Robots and Systems*, Vol. 3, 2004, pp. 2451-2456.

[4] Tayebi, A. and McGilvray, S., "Attitude Stabilization of a VIOL Quadrotor Aircraft", *IEEE Transaction on Control Systems Technology*, Vol. 14, No. 3, 2006, pp. 562-571.

[5] Erginer, B. and Altug, E., "Modeling and PD Control of a Quadrotor VTOL Vehicle", *Proc. of the IEEE Intelligent Vehicles Symposium*, 2007, pp. 894-899.

[6] Chen, X., Li, D., Bai, Y. and Xu, Z., "Modeling and Neuro-fuzzy Adaptive Attitude Control for Eight-rotor MAV", *International Journal of Control, Automation and Systems*, Vol. 9, No. 6, 2011, pp. 1154-1163.

[7] Chen, X. J. and Li, D., "Modeling and Designing Intelligent Adaptive Sliding Mode Controller for an Eight-Rotor MAV", *International Journal of Aeronautical and Space Sciences*, Vol. 14, No. 2, 2013, pp. 172-182.

[8] Melin, P. and Castillo, O., "A New Method for Adaptive Model-based Control of Non-linear Dynamic Plants Using a Neuro–fuzzy–fractal Approach", *Soft Computing Journal*, Vol. 5, No. 2, 2001, pp. 171–177.

[9] Lou, X., Sun, Z. and Sun, F., "A New Approach to Fuzzy Modeling and Control for Nonlinear Dynamic Systems: Neuro-Fuzzy Dynamic Characteristic Modeling and Adaptive Control Mechanism", *International Journal of Control, Automation, and Systems*, Vol. 7, No. 1, 2009, pp. 123-132.

[10] Melin, P. and Castillo, O., "Intelligent Control of Complex Electrochemical Systems with a Neuro–fuzzy–genetic Approach", *IEEE Transactions on Industrial Electronics*, Vol. 48, No. 5, 2001, pp. 951–955.

[11] Er, M. J., Low, C. B., Nah, K. H., Lim, M. H. and Ng, S. Y., "Real-time Implementation of a Dynamic Fuzzy Neural Networks Controller for a SCARA", *Microprocessors and Microsystems*, Vol. 26, No. 9, 2002, pp. 449-461.

[12] Lee, C. H., Lin, Y. C. and Lai, W. Y., "Systems Identification Using Type-II Fuzzy Neural Network (type-II FNN) Systems", *In Proc. IEEE Int. Symp. Comput. Intell.* Robot. Antom., Vol. 3, 2003, pp. 1264-1269.

[13] Wang, C. H., Cheng, C. S. and Lee, T. T., "Dynamic Optimal Training for Interval Type-II Fuzzy Neural Network (T2FNN)", *IEEE Trans. Syst., Man, Cybern. B*, Vol. 34, No. 3, 2004, pp. 1462-1477.

[14] Tsung-Chih Lin. Based on interval type-II fuzzy-neural network direct adaptive sliding mode control for SISO nonlinear systems. Communications in Nonlinear Science and Numerical Simulation, 2010,15:4084-4099

[15] Faa-Jeng Lin, Po-IIuan Chou. Adaptive control of two-axis motion control system using interval type-II fuzzy neural network. *IEEE Transactions on Industrial Electronics*. 2009; 56: 178-193.

[16] Lin, F. J., Chou, P. H., Shieh, P. H. and Chen, S. Y., "Robust Control of an LUSM-based x-y-tha Motion Control Stage Using an Adaptive Interval Type-II Fuzzy Neural Network", *IEEE Transactions on Fuzzy Systems*, Vol. 17, No. 1, 2009, pp. 24-38.